All possible ternary fragmentations of ^{252}Cf in collinear configuration

K. Manimaran and M. Balasubramaniam*
Department of Physics, Bharathiar University, Coimbatore 641046, India
(Received 29 August 2010; revised manuscript received 17 December 2010; published 21 March 2011)

All possible ternary fragmentations in fission of ^{252}Cf are studied in collinear configuration within a spherical approximation using the recently proposed "three cluster model." The potential energy surface of collinear configuration exhibits a strong valley around ^{48}Ca and its neighboring nuclei ^{50}Ca, ^{54}Ti, and ^{60}Cr. Such strong minima are not seen in the potential energy surface of an equatorial configuration. As a consequence of strong minima in the potential, the overall relative yield is higher for the ternary fragmentation with ^{48}Ca, ^{50}Ca, ^{54}Ti, ^{60}Cr, and ^{82}Ge as the third fragment. The results of potential energy and relative yield calculations reveal that collinear configuration increases the probability of emission of heavy fragments like ^{48}Ca (doubly magic nucleus) and its neighboring nuclei as the third fragment. The obtained results indicate that the collinear configuration is the preferred configuration for intermediate nuclei (^{48}Ca, ^{50}Ca, ^{54}Ti, and ^{60}Cr) as the third fragment in particle accompanied fission while the equatorial configuration may be a preferred configuration for light nuclei (^{4}He, ^{10}Be) as the third fragment.

DOI: 10.1103/PhysRevC.83.034609 PACS number(s): 25.85.Ca, 21.60.Gx

I. INTRODUCTION

The breakup of a radioactive nucleus into three fragments covers a spectrum of fission events from one end in which a scission neutron accompanies two main fission fragments to the other end in which three fragments of about equal masses are emitted. The ternary fission process with three charged particles in the outgoing channel, the third particle being very light compared to the main fission fragments situated between these two extremes, is called light charged particle (LCP) accompanied fission. The spontaneous breakup into three nuclei of about equal masses called true ternary fission has not yet been observed experimentally but is theoretically being investigated. At the same time, in induced reactions there exists a signature of true ternary fission as reported in Refs. [1–5]. Rosen and Hudsen [1] reported a yield of 6.7 ± 3.0 per 10^6 binary fission in the induced fission of ^{235}U by thermal neutrons. Fleischer *et al.* [2] measured the cross section for both binary (3.0 ± 0.4 b) and true ternary fissions (1/30$^{\text{th}}$ of binary) in the reaction Ar (400 MeV) + Th. In the induced fission of ^{238}U by intermediate-energy (20–120 MeV) helium ions, Iyer and Cobble [3] presented evidence for the existence of a true ternary fission by measuring the absolute cross section of the fragments ^{24}Na, ^{28}Mg, ^{31}S, ^{38}S, ^{47}Ca, ^{56}Mn, and ^{56}Ni. Perelygin *et al.* [4] used Ar (230–380 MeV) projectiles to study the ternary fission of Au, Bi, Th, and U, in which the angular distributions and the length of the fission tracks are reported. Becker *et al.* [5] measured a high ternary (true ternary fission) to binary ratio of $4.3 \pm 0.7\%$, in the case of uranium irradiated with 540-MeV Fe ions, and reported that ternary fission increases with the use of projectiles heavier than Ar. Very asymmetric ternary fission is a competing decay mode with binary fission and is observed in spontaneous [6–11] and induced [12–15] ternary fissions. The most observed LCP (about 90%) accompanying ternary fission is the α particle, preferentially emitted in a direction orthogonal to the fission axis. The angular distribution of these LCPs accompanying the ternary fission reveals that they are formed in the neck region between the two main fission fragments and emitted in a direction perpendicular to the fission axis as a result of high Coulombic force. The ternary fission process in which the third fragment is emitted in a direction perpendicular to the fission axis, is termed as equatorial or orthogonal emission and if the third fragment is emitted in the direction of fission axis along with the other two fragments is termed as collinear or polar emission.

From three independent experiments Pyatkov *et al.* [16,17] has recently reported a new island of high yields of ^{252}Cf(sf) collinear cluster tripartition (CCT) in the fragment mass space. The true ternary spontaneous decay channel observed/reported as CCT from these experiments having masses close to the magic ^{132}Sn, ^{70}Ni, and ^{48}Ca isotopes has a probability of not less than 4×10^{-3} with respect to binary fission. This is larger than the known ternary fission accompanied by LCPs. They also observed the same CCT in the induced reaction ^{235}U(n_{th}, f). von Oertzen *et al.* [18–20] observed collinear ternary cluster decay (or ternary fission) of hyperdeformed light compound nuclei ^{56}Ni* and ^{60}Zn* formed in the reactions ^{32}S + ^{24}Mg ($E_{\text{lab}} = 165.4$ MeV) and ^{36}Ar + ^{24}Mg ($E_{\text{lab}} =$ 195 MeV), respectively. In these experiments the collinear ternary cluster decay process is described as the decay of hyperdeformed states with large angular momenta around 45–52 $\hbar$. Herbach *et al.* [21] studied the ternary fission of heavy hot composite systems with excitation energies of 1.5–2.5 MeV/amu in the reactions of ^{14}N with ^{197}Au and ^{232}Th and reported that the ternary decay cross section decreases from 5 to 0.08 mb (^{14}N + ^{197}Au) and from 15 to 0.8 mb (^{14}N + ^{232}Th), respectively, while the charge number of the emitted lightest fragment (Z_3) increases from 6 to 25. In this experiment, the mass, energy, charge number of fragments with $Z < 25$ and the velocity vectors of these fragments in the range of 1.54 cm/ns are measured.

On theoretical grounds there are different models [22–31] to explain the ternary fission process to calculate relative isotopic

*m.balou@gmail.com

yield, to find the existence of long-living trinuclear molecules, and to predict favored ternary splittings. Royer *et al.* [32] estimated the ternary potential barrier for three nuclei, viz., ^{56}Fe, ^{149}Eu, and ^{240}Pu, in three different modes, namely, prolate (collinear emission), oblate (equatorial emission), and cascade ternary fissions within the rotational liquid drop model at finite temperature including the nuclear proximity energy. This barrier calculation reveals that in all the three nuclei (^{56}Fe, ^{149}Eu, and ^{240}Pu) oblate fission (equatorial emission) barriers are the highest (less probable). For ^{56}Fe nuclei the cascade fission is favored while for the nuclei ^{149}Eu and ^{240}Pu the prolate ternary fission (collinear emission) becomes the most probable. In Ref. [33] the ternary fission barrier for ^{48}Ca leading to the systems $^{16}\mathrm{O} + {}^{16}\mathrm{O} + {}^{16}\mathrm{O}$ and $^{20}\mathrm{Ne} + {}^{8}\mathrm{Be} + {}^{20}\mathrm{Ne}$ through prolate ternary configuration (collinear configuration) is studied and it is reported that the existence of $^{16}\mathrm{O} + {}^{16}\mathrm{O} + {}^{16}\mathrm{O}$ molecular state seems to be possible at intermediate spins.

Poenaru *et al.* [34] studied the existence of quasinuclear molecules during the continuous deformation that leads to particle accompanied fission of ^{252}Cf, based on a liquid drop model assuming that the third light particle is formed collinearly in between the main fission fragments, when the neck radius becomes equal to the radius of the third fragment. Further it was reported that there appears a minimum in the deformation energy in the region between the neck formation and the touching configuration of the three fragments that lie collinearly on the fission axis. Poenaru *et al.* [35], also studied the multicluster accompanied fission of ^{252}Cf by assuming that the lighter fragments are formed collinearly in between the main fission fragments and reported that this collinearly aligned configuration has optimum configuration in multicluster accompanied fission. Cseh *et al.* [36–39] studied the allowed and forbidden binary and ternary clusterizations. They carried out the study in light (^{36}Ar), medium, and heavy (^{252}Cf) nuclei in their ground, superdeformed, and hyperdeformed states based on the energy minimum principle (summed differences of the measured binding energies and the corresponding liquid drop values) and the Pauli exclusion principle. The exclusion principle is taken into account by a selection rule based on symmetries (microscopic nuclear structure) of the fragments. The U(3) symmetry is adopted for light nuclei which is a good approximation for light nuclei and the effective or quasidynamical U(3) symmetry is adopted for medium and heavy nuclei due to the importance of the symmetry breaking interactions, like spin orbit and pairing. It was stated in Refs. [38,39] that the energetic stability and the exclusion principle have different preferences for possible configurations. All these experimental observations and theoretical predictions suggest that collinear emission is more probable at least for heavy third fragments than equatorial emission.

Recently a new model called the "three cluster model" (TCM) has been proposed by us [40] to study the ternary fission of heavy radioactive nuclei. Using the TCM within a spherical approximation, the equatorial emission of α particles as the third fragment in the ternary fission of ^{252}Cf is studied and the yields are compared with the experimental results of Ramayya *et al.* [7]. Later, deformation and orientation degrees of freedom are introduced [41] within the TCM, and LCP (^{4}He and ^{10}Be) accompanied fission of ^{252}Cf is studied in which the most probable ternary configurations with ^{4}He and ^{10}Be as the third fragment are predicted. Very recently [42] equatorial emission of all possible third fragments from the ternary fission of ^{252}Cf is investigated using the TCM and the most probable ternary configurations with all possible third fragment mass numbers from $A_3 = 1$ to 84 are predicted. In all these studies the energy minimization principle alone is considered. In this work collinear emission of all possible ternary fragments in fission of ^{252}Cf is studied within a spherical approximation using the TCM.

II. THREE CLUSTER MODEL (TCM)

The three cluster model (TCM) [40–42] has been recently developed to explain the ternary fission of heavy radioactive nuclei based on the cluster picture. Within this model for a fixed third fragment, one can calculate the fragmentation potential minimized in mass and charge asymmetry coordinates and one can study systematically the probability of fragments and isotopic yield of ternary fission of given nucleus. The fragmentation potential is defined in the TCM as

$$V_{\mathrm{tot}} = \sum_{i=1}^{3} \sum_{j>i}^{3} (B_i + V_{ij}), \tag{1}$$

where B_i are the binding energies of the three fragments in energy units, taken from Refs. [43,44], and

$$V_{ij} = V_{Cij} + V_{Nij}. \tag{2}$$

Here $V_{Cij} = Z_i Z_j e^2 / R^s_{ij}$, the Coulomb interaction between the three nuclei with $R^s{}_{ij} = R_{ij} + s_{ij}$, where R^s_{ij} is the distance between the centers of the interacting fragments. R_{ij} is the sum of the radii of interacting fragments and s_{ij} is the surface separation distance between the fragments. R_{ij} is defined as $R_{12} = R_1 + R_2$, $R_{13} = R_1 + R_3$, $R_{23} = R_2 + R_3$, with $R_i = r_0 \times A_i^{1/3}$, $r_0 = 1.16$ fm; and the separation distances for the equatorial configuration are considered as

$$s_{12} = s_{13} = s_{23} = s \tag{3}$$

and for the collinear configuration are considered as

$$s_{12} = s_{23} = s \quad \text{and} \quad s_{13} = 2(R_2 + s), \tag{4}$$

with $s = 0$ corresponding to the touching configuration of three fragments as shown in Figs. 1(a) and 1(b), respectively. In collinear configuration the second fragment is considered to lie in between the first and the third fragment. V_{Nij} is the short-range Yukawa plus exponential nuclear attractive potential among the three fragments and is defined as

$$V_{Nij} = -4\left(\frac{a}{r_0}\right)^2 \sqrt{a_{2i} a_{2j}} \times [g_i g_j (4 + \xi) - g_j f_i - g_i f_j] \frac{\exp(-\xi)}{\xi}, \tag{5}$$

where $\xi = R^s_{ij}/a$, and the functions g and f are

$$g_k = \zeta \cosh \zeta - \sinh \zeta \tag{6}$$

and

$$f_k = \zeta^2 \sinh \zeta, \tag{7}$$

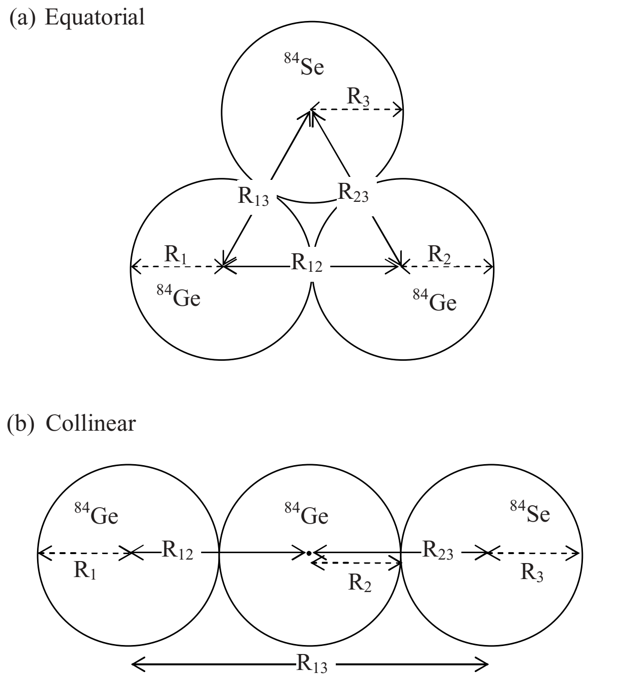

FIG. 1. Schematic touching configurations of three spherical nuclei (a) in the case of equatorial emission and (b) in the case of collinear emission.

where $\zeta = R_i/a$ and $a = 0.68$ fm is the diffusivity parameter and the asymmetry parameter $a_{2k} = a_s(1 - \omega I^2)$, with $a_s = 21.13$ MeV, $\omega = 2.3$, and $I = \frac{N-Z}{A}$. The three-body barrier penetration probability (P) of a given fragmentation is defined by the WKB integral as in Ref. [40],

$$P = \exp\left[-\frac{2}{\hbar}\int_{s_1}^{s_2}\{2\mu_{123}[V(s) - Q]\}^{1/2} ds\right], \quad (8)$$

where $V(s)$ is the sum of the Coulomb potential (V_{Cij}) plus the nuclear attractive potential (V_{Nij}) as given in Eq. (2) and it is calculated by varying the surface separation distance s as given in Eqs. (3) and (4) corresponding to equatorial and collinear configuration. Q is the available energy for three decay products and is defined in the model as

$$Q = M - \sum_{i=1}^{3} m_i, \quad (9)$$

where M is the mass excess of the decaying nucleus and m_i are the mass excesses of the product nuclei. In the case of collinear emission, the available Q value is shared by the first and third fragments ($Q = E_1 + E_3$), assumed to be moving in opposite directions among the three decay products and the second fragment is considered at rest ($E_2 = 0$). μ_{123} is the reduced mass of the three fragments and it is defined as

$$\mu_{123} = \left(\frac{\mu_{12}A_3}{\mu_{12} + A_3}\right)m, \quad (10)$$

where m is the nucleon mass and

$$\mu_{12} = \frac{A_1 A_2}{A_1 + A_2}. \quad (11)$$

The relative yields for all the charge minimized fragmentation channels are calculated as the ratio between the penetration probability of a given fragmentation over the sum of penetration probabilities of all possible fragmentations as

$$Y(A_i, Z_i) = \frac{P(A_i, Z_i)}{\sum P(A_i, Z_i)}. \quad (12)$$

Here $P(A_i, Z_i)$ is the same as the penetration probability as defined in Eq. (8) corresponding to a given fragmentation; here A_i denotes $A_1 + A_2 + A_3$ and Z_i denotes $Z_1 + Z_2 + Z_3$ (these are minimized charges as labeled in Fig. 5 as ^{132}Sn + ^{72}Ni + ^{48}Ca).

III. RESULTS AND DISCUSSION

The ternary fragmentation potential in touching configuration for collinear configuration of fragments, within a spherical approximation and satisfying the condition $A_1 \geqslant A_2 \geqslant A_3$, is calculated for ^{252}Cf with third fragment mass numbers from $A_3 = 1$ to 84. For all the possible 84 third fragment masses the potential energy is minimized with respect to their charge asymmetry as in Refs. [40–42]. For example, for $A_3 = 48$, one has 12 possible charge numbers from $Z_3 = 16$ to $Z_3 = 27$, leaving the remaining system from ^{204}Pb to ^{204}Yb whose binary fragmentation ($A_1 + A_2$) is minimized in charge asymmetry coordinate η_z. In Fig. 2 among these 12 possible $A_3 = 48$ fragments we present the ternary fragmentation potentials of even Z_3 fragments from $Z_3 = 16$ to $Z_3 = 24$ (for the sake of clarity) in collinear touching configuration

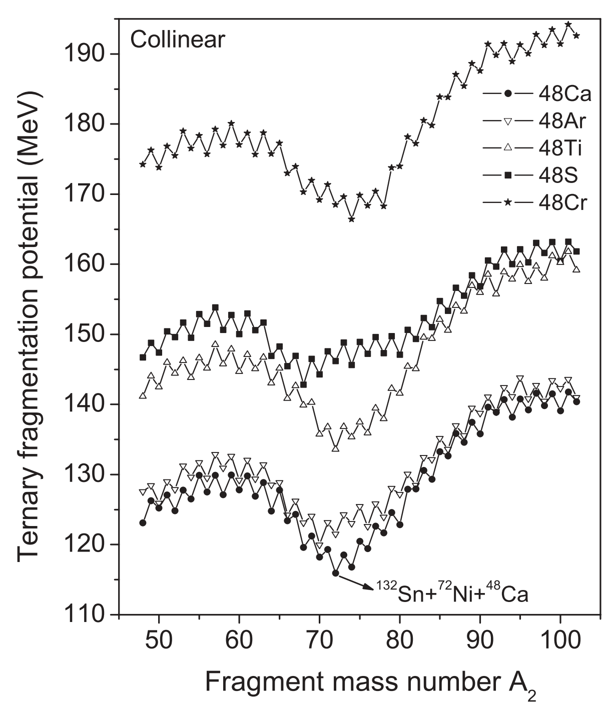

FIG. 2. The ternary fragmentation potential for collinear emission of fragments in ternary fission of ^{252}Cf nucleus for different third fragments with mass number $A_3 = 48$ plotted as a function of fragment mass number A_2.

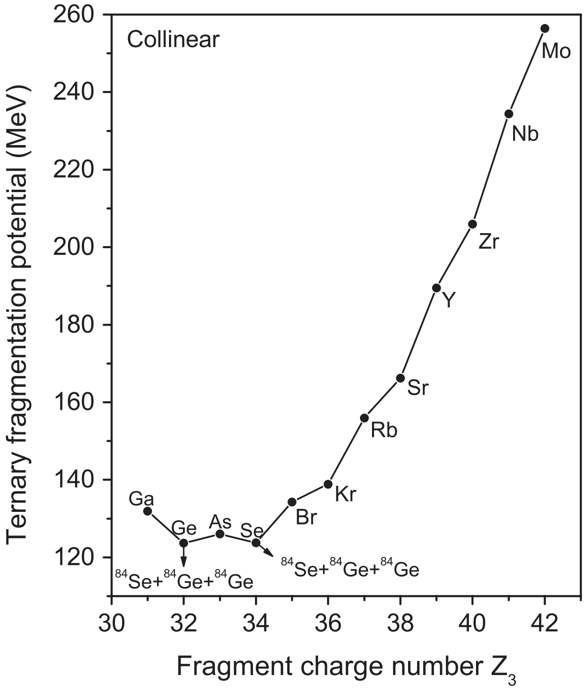

FIG. 3. The ternary fragmentation potential for collinear emission of fragments in ternary fission of ^{252}Cf nucleus for different third fragments with mass number $A_3 = 84$ plotted as a function of fragment charge number Z_3.

as a function of fragment mass number A_2. Among the 12 possible third fragments the PES corresponding to ^{48}Ca (solid circle connected by solid line) lies the lowest, and particularly the fragment combination ^{132}Sn + ^{72}Ni + ^{48}Ca has minimum potential. This is due to the effect of the doubly magic nuclei ^{132}Sn ($Z = 50$, $N = 82$) and ^{48}Ca ($Z = 20$, $N = 28$) and the proton magic nucleus ^{72}Ni in this fragment combination. The same fragment combination is observed with maximum yield in the CCT of ^{252}Cf in recent experiments [16,17].

In another example (true ternary fission) for the mass 84 nucleus ($A_3 = 84$), one has 12 possible charge numbers from 31 to 42, leaving the remaining system from ^{168}Ho to ^{168}Ba whose binary fragmentation ($A_1 + A_2$) is minimized in charge asymmetry coordinate η_z. While satisfying the condition $A_1 \geqslant A_2 \geqslant A_3$ only one mass asymmetry is possible, i.e., $A_1 = 84$ and $A_2 = 84$, whose charge minimization with respect to their charge asymmetry is considered. The resulting ternary fragmentation potential in collinear touching configuration for the third fragments with mass number $A_3 = 84$ is presented in Fig. 3 as a function of third fragment charge number Z_3. Among the 12 possible fragment configurations the ^{84}Se + ^{84}Ge + ^{84}Ge configuration has the minimum potential. This is due to the neutron closed shell ($N = 50$) effect in all the three fragments. It was already shown by us in Refs. [40,42], that among the three preferred fragments in ternary fission, at least one (or two) of the fragments or all the three fragments associate with the neutron (or proton) closed shell and in some cases even with the doubly closed shell nucleus. In this figure, the two configurations marked by an arrow, viz., ^{84}Se + ^{84}Ge + ^{84}Ge and ^{84}Ge + ^{84}Ge + ^{84}Se, are equally probable since the fragments are the same, except for their order.

The ternary fragmentation potentials minimized with respect to their mass and charge asymmetry coordinates in equatorial and collinear touching configurations for all the possible fragments with $A_3 = 1$ to 84, in the fission of ^{252}Cf, are presented as a function of third fragment mass number A_3 in Figs. 4(a) and 4(b), respectively. In the collinear

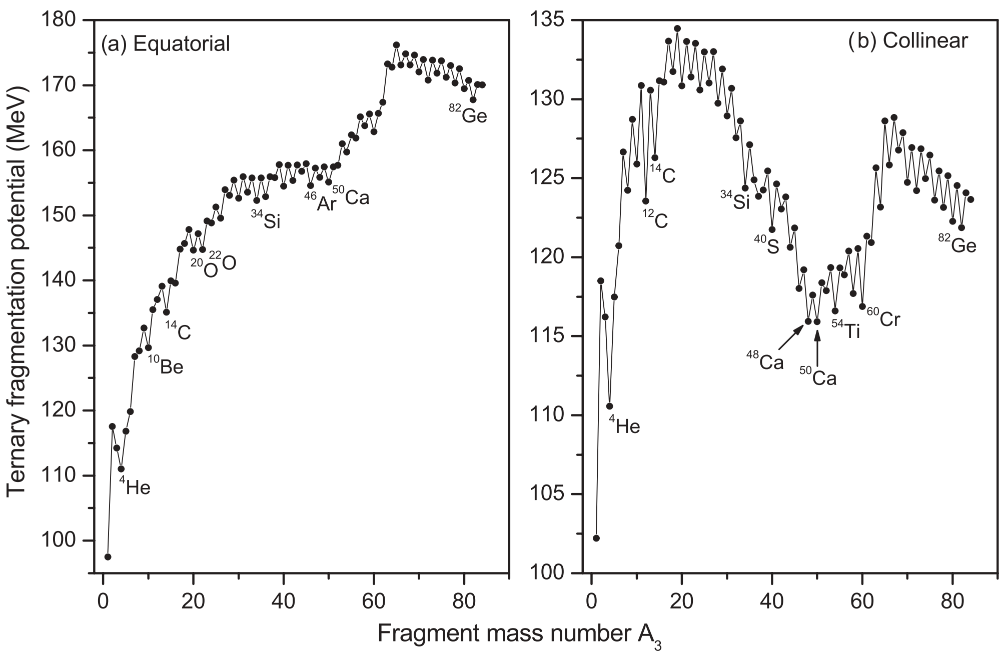

FIG. 4. A comparison between the mass and charge minimized ternary fragmentation potential of the most probable configuration in (a) equatorial and (b) collinear emission of fragments in the ternary fission of ^{252}Cf for $A_3 = 1$ to 84 plotted as a function of third particle mass number A_3.

configuration a strong valley is seen in the potential energy surface corresponding to the third fragments Ca through Cr that is not present in the potential energy surface of equatorial configuration. For the ternary configurations with ^{48}Ca, ^{50}Ca, ^{54}Ti, and ^{60}Cr as third fragments, the potential energy lies lower than the most probable LCPs (^{10}Be and ^{14}C) observed next to the ^{4}He in the ternary fission of ^{252}Cf. There is a large difference in the magnitude of potential energy between collinear and equatorial configurations; particularly in the case of true ternary fission it is around 45 MeV. This is due to the fact that there will be a reduction in the Coulombic potential between the first and the third fragment because of the large interfragment distance. The effect of this will be very high for heavy fragments due to their larger charges. This implies that ternary fission with heavy third fragments and symmetric ternary fission prefer collinear emission.

The scattering potential is calculated from Eq. (1) considering only the interaction potential (without binding energies) between the fragments by increasing the value of surface separation s as in equations Eqs. (3) and (4) for equatorial and collinear emissions, respectively. In the case of collinear emission, surface separations between fragments 1 and 2 as well as between 2 and 3 are varied uniformly and hence the interfragment distance between fragments 1 and 3 varies automatically. The calculated scattering potential for the mass and charge minimized fragment combination ^{132}Sn + ^{72}Ni + ^{48}Ca is plotted as a function of s in Fig. 5. The potential barrier height for collinear emission is approximately 57 MeV lower than the barrier for equatorial emission and this emphasizes that collinear emission is more preferred than equatorial emission. Figures 6 and 7 present the barrier height and the corresponding barrier position for all possible mass and charge minimized ternary fragmentations with $A_3 = 1$

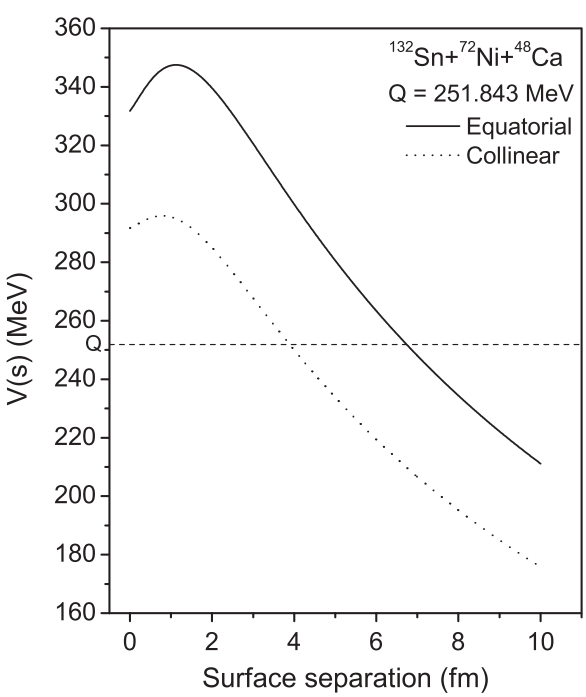

FIG. 5. The scattering potential for equatorial and collinear emission of fragmentation ^{132}Sn + ^{72}Ni + ^{48}Ca in ternary fission of a ^{252}Cf nucleus plotted as a function of surface separation.

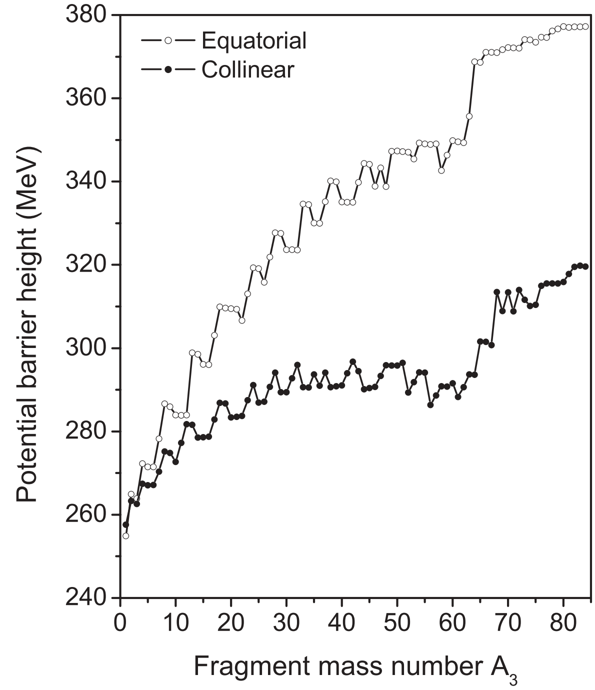

FIG. 6. The potential barrier height for all possible mass and charge minimized ternary fragmentations corresponding to equatorial and collinear emission of ^{252}Cf nucleus plotted as a function of fragment mass number A_3.

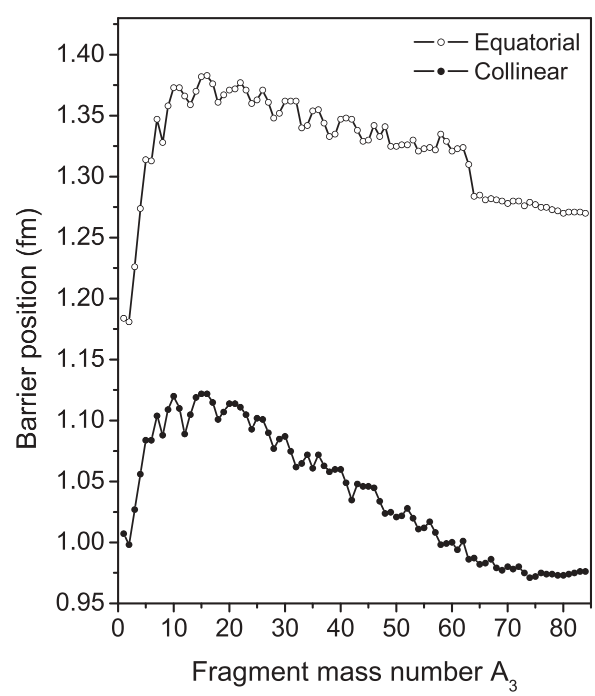

FIG. 7. The potential barrier position for all possible mass and charge minimized ternary fragmentation corresponding to equatorial and collinear emission of a ^{252}Cf nucleus is plotted as a function of fragment mass number A_3.

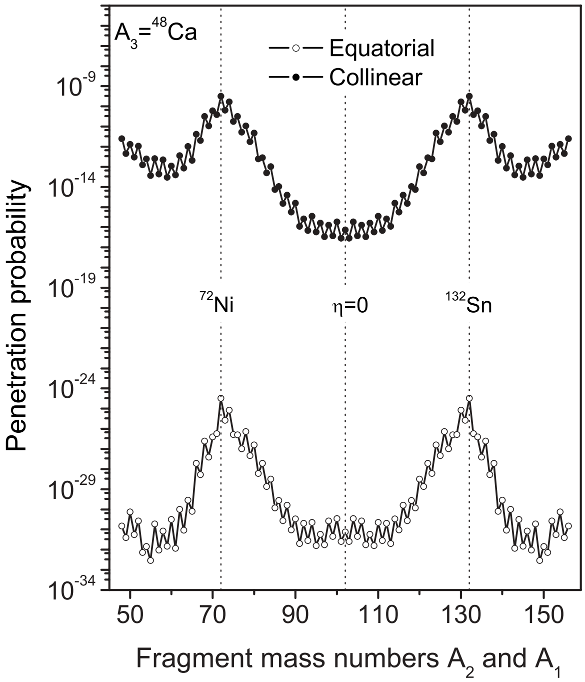

FIG. 8. The penetration probability calculated for equatorial and collinear emission of fragments in ternary fission of a ^{252}Cf nucleus for fixed third fragment $A_3 = {}^{48}$Ca.

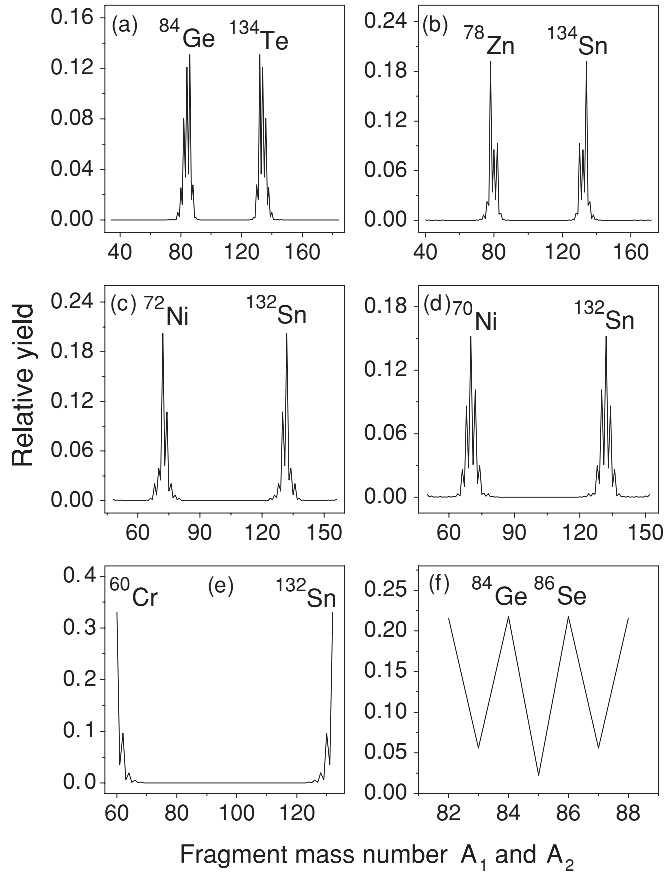

FIG. 9. The individual relative yields of different charge minimized ternary fragmentation with $A_3 = {}^{34}$Si, ^{40}S, ^{48}Ca, ^{50}Ca, ^{60}Cr, and ^{82}Ge are plotted as a function of fragment mass number (A_2) in panels (a), (b), (c), (d), (e), and (f), respectively. The most probable configurations A_1 and A_2 are labeled.

to 84, both in the equatorial and the collinear configuration. The barrier height in the collinear configuration of $A_3 > 3$ lies lower than the corresponding barrier height in the equatorial configuration. Particularly for the heavy fragments the difference is larger. Hence for heavy fragments collinear configuration seems to be more probable than equatorial configuration. Similarly, the barrier position in collinear configuration is lower than that in equatorial configuration for all configurations. Figure 8 presents the comparison between penetration probability calculated in equatorial and collinear configurations of the fragments as a function of fragment mass numbers A_1 and A_2. In other words as a function of mass asymmetry $\eta = (A_1 - A_2)/(A_1 + A_2)$ between the fragments $A_1$and A_2 (the third fragment mass number is fixed), $\eta = 0$ corresponding to $A_1 = A_2$ is also shown. The mass number in the horizontal axis, toward the left and right side of $\eta = 0$, corresponds to the light fragment mass number A_2 and the heavy fragment mass number A_1, respectively. Penetration probability in the collinear emission is higher by 15 orders of magnitude than in the equatorial emission, which indicates the preference of collinear emission over equatorial emission. In both the configurations the fragmentation ^{132}Sn + ^{72}Ni + ^{48}Ca has the maximum penetration probability.

The relative yields of all possible ternary fragmentation of ^{252}Cf are calculated as defined in Eq. (12). In Fig. 9, individual relative yields are plotted as a function of fragment mass numbers A_1 and A_2 for a few selected third fragments ^{34}Si, ^{40}S, ^{48}Ca, ^{50}Ca, ^{60}Cr, and ^{82}Ge. The individual relative yield is the ratio between the penetration probability of a given fragmentation over the sum of penetration probabilities of all possible fragmentations for fixed third fragments [i.e., the penetration probabilities of all possible fragmentations for a particular third fragment alone is summed to give $\sum P(A_i, Z_i)$]. In this figure each panel corresponds to different third fragments and the yield is calculated for each third fragment with respect to other possible fragmentations. Hence one should not compare the magnitude of the individual relative yield corresponding to a particular third fragment with the relative yield of other third fragments as well as with that of the results obtained in equatorial emission [42].

Figure 10 presents the overall relative yield for all the possible cases ($A_3 = 1$ to 84) as a function of third fragment mass number A_3. The overall relative yield is the ratio between the penetration probability of a given fragmentation over the sum of penetration probabilities of all possible fragmentations corresponding to A_3 from 1 to 84 [i.e., the penetration probabilities of all possible fragmentation with A_3 from 1 to 84 are summed to give $\sum P(A_i, Z_i)$]. Here the yield of a particular fragment combination is calculated relative to all the other possible ternary fragmentations of ^{252}Cf and hence one can compare the yield of one fragmentation with the other. The hatched and black histograms in this figure correspond to the third fragments with odd and even mass numbers, respectively. The third fragments with even mass number

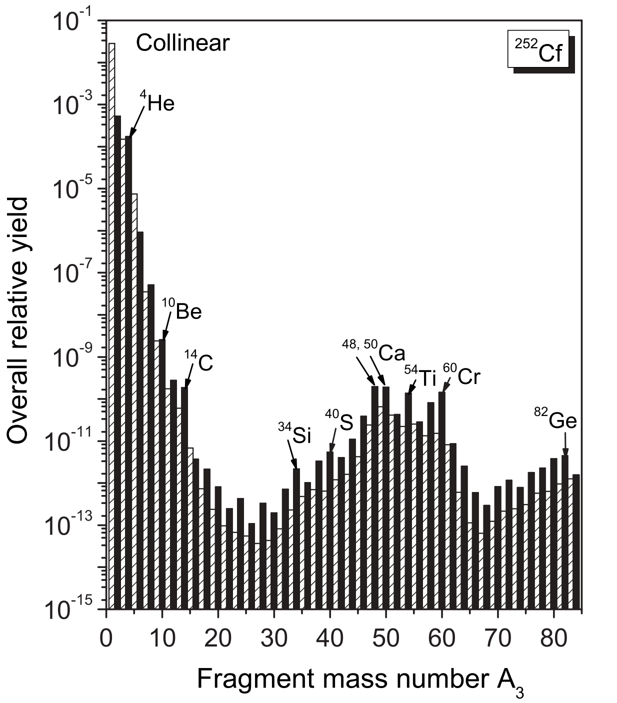

FIG. 10. The overall relative yields of the ternary fission fragmentation of ^{252}Cf, accompanied with all possible charge minimized third fragments $A_3 = 1$ to 84 plotted as a function of third fragment mass number A_3.

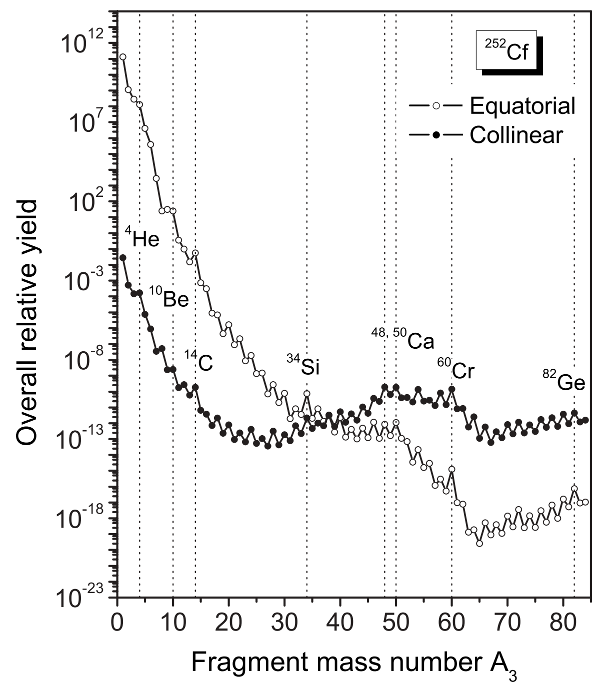

FIG. 11. A comparison between the overall relative yield calculated for equatorial and collinear emission of fragments in ternary fission of ^{252}Cf plotted as a function of third fragment mass number A_3.

have relatively larger yields compared to the odd ones. As a consequence of deep minimum in the fragmentation potential for the fragmentation with $A_3 = {}^{48}$Ca, ^{50}Ca, ^{54}Ti, and ^{60}Cr, the overall relative yields for these fragmentations are relatively larger than their neighboring ones. It is to be mentioned here that, though ^{10}Be and ^{14}C are shown to have potential energy larger than that of ^{48}Ca, ^{50}Ca, ^{54}Ti, and ^{60}Cr, the overall relative yield of ^{10}Be is larger than these third fragments and for ^{14}C the magnitude of the yield is of the same order. The yield corresponding to the symmetric ternary fission also shoots up and particularly ^{82}Ge has larger magnitude in this mass region.

For a better comparison we present in the Fig. 11 the overall relative yield calculated in equatorial and collinear configurations in ternary fission of ^{252}Cf as a function of third fragment mass number A_3. The relative yield corresponding to equatorial emission of third fragment lies above the relative yield corresponding to the collinear emission of fragments up to third fragments with mass number $A_3 = 38$. Beyond that the yield corresponding to collinear emission lies well above the relative yield of equatorial emission. This result indicates that light third fragments prefer the equatorial emission and the heavy third fragments prefer the collinear emission. In particular the relative yield corresponding to the fragment ^{48}Ca and its neighboring nuclei is larger in collinear emission. It is relevant to mention here that in a recent experiment [16,17], CCT of ^{252}Cf was observed with a large probability (4×10^{-3} with respect to binary fission), with doubly magic ^{48}Ca, and with its neighboring nuclei as the third fragment. To further strengthen the argument we present in Fig. 12 the comparison of our calculated individual relative yield with experimental yields (black histograms) for the α accompanied fission of ^{252}Cf corresponding to both the

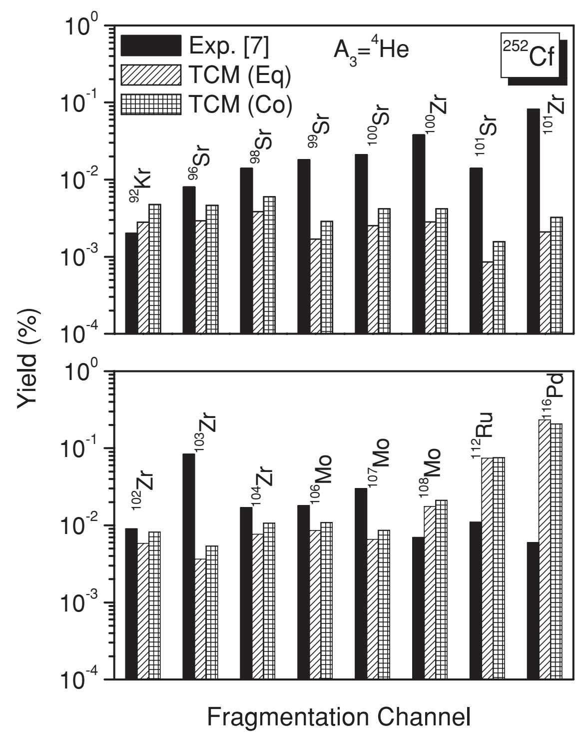

FIG. 12. The relative yield calculated for equatorial and collinear emission of fragments in α accompanied fission of ^{252}Cf are compared with the experimental data.

equatorial (hatched histograms) and the collinear emission (checked histograms). The results indicate that both the configurations seem to be probable for α accompanied fission with collinear configuration having slightly higher value than equatorial emission for all the 16 cases computed. However it must be mentioned here that this result of independent relative yield should not be compared directly with the overall relative yield calculation as presented in Fig. 11 for the equatorial and collinear configurations.

IV. SUMMARY

Collinear emission of all possible ternary fragments from the fission of ^{252}Cf is studied within a spherical approximation based on the recently [40] proposed TCM. In the collinear configuration a new strong valley appears in the mass and charge minimized ternary fragmentation potential for the ternary fragment combinations with ^{48}Ca and its neighboring nuclei ^{50}Ca, ^{54}Ti, and ^{60}Cr as third fragments, which was not found in the potential calculated in equatorial emission. Apart from this, another minimum appears in the ternary fragmentation potential for the symmetric mass region. The overall relative yield is calculated in the collinear emission of all possible third fragments and compared with the overall relative yield calculated in the equatorial emission. The overall relative yield corresponding to the equatorial emission of the third fragment lies above the overall relative yield corresponding to the collinear emission of fragments up to third fragments with mass number $A_3 = 38$, and beyond that the overall relative yield corresponding to collinear emission increases. As a consequence of the fragmentation potential, the overall relative yield particularly for the ternary fragment combinations with ^{48}Ca, ^{50}Ca, ^{54}Ti ^{60}Cr, and ^{82}Ge in collinear configuration shoots up in magnitude. The overall relative yields corresponding to these fragments are of the same order of ^{14}C, the most observed third fragment in ternary fission of ^{252}Cf next to ^{4}He and ^{10}Be. The results of overall relative yield for all the third fragments reveal that the light third fragments prefer the equatorial emission while the heavy third fragments prefer the collinear emission. The results of individual relative yield of a particular third fragment, ^{4}He, in ternary fission of ^{252}Cf indicates a preference for both the configurations, with the collinear configuration having a slight edge over the equatorial configuration with respect to the experimentally measured yields.

ACKNOWLEDGMENTS

The author MB acknowledges the financial support in the form of project supported by the Board of Research in Nuclear Science, see letter No. 2009/36/40-BRNS/1691 dated 17/09/2009.

[1] L. Rosen and A. M. Hudson, Phys. Rev. **78**, 533 (1950).
[2] R. L. Fleischer, P. B. Price, R. M. Walker, and E. L. Hubbard, Phys. Rev. **143**, 943 (1966).
[3] R. H. Iyer and J. W. Cobble, Phys. Rev. **172**, 1186 (1968).
[4] V. P. Perelygin, N. H. Shadieva, S. P. Tretyakova, A. H. Boos, and R. Brandt, Nucl. Phys. A **127**, 577 (1969).
[5] H. J. Becker, P. Vater, R. Brandt and A. H. Boos, Phys. Lett. B **50**, 24 (1974).
[6] P. Singer, M. Mutterer, Yu. N. Kopatch, M. Klemens, A. Hotzel, D. Schwalm, P. Thirolf, and M. Hesse, Z. Phys. A **359**, 41 (1997).
[7] A. V. Ramayya *et al.*, Nuovo Cimento A **110**, 1073 (1997); Phys. Rev. C **57**, 2370 (1998).
[8] A. V. Ramayya *et al.* (GANDS95 Collabration.), Phys. Rev. Lett. **81**, 947 (1998).
[9] U. Köster, H. Faust, G. Fioni, T. Friedrichs, M. Groß, and S. Oberstedt, Nucl. Phys. A **595**, 371 (1999).
[10] Yu. N. Kopatch, M. Mutterer, D. Schwalm, P. Thirolf, and F. Gonnenwein, Phys. Rev. C **65**, 044614 (2002).
[11] A. V. Daniel *et al.*, Phys. Rev. C **69**, 041305(R) (2004).
[12] G. Kugler and W. B. Clarke, Phys. Rev. C **5**, 551 (1972).
[13] C. Wagemans, P. D'hondt, P. Schillebeeckx, and R. Brissot, Phys. Rev. C **33**, 943 (1986).
[14] F. Gönnenwein, A. Möller, M. Cröni, M. Hesse, M. Wöstheinrich, H. Faust, G. Fioni, and S. Oberstedt, Nuovo Cimento A **110**, 1089 (1997).
[15] I. Tsekhanovich, Z. Büyükmumcu, M. Davi, H. O. Denschlag, F. Gönnenwein, and S. F. Boulyga, Phys. Rev. C **67**, 034610 (2003).
[16] Yu. V. Pyatkov *et al.*, Rom. Rep. Phys. **59**, 569 (2007).
[17] Yu. V. Pyatkov *et al.*, Eur. Phys. J. A **45**, 29 (2010).
[18] W. von Oertzen *et al.*, Eur. Phys. J. A **36**, 279 (2008).
[19] W. von Oertzen, V. Zherebchevsky, B. Gebauer, Ch. Schulz, S. Thummerer, D. Kamanin, G. Royer, and Th. Wilpert, Phys. Rev. C **78**, 044615 (2008).
[20] W. von Oertzen *et al.*, J. Phys.: Conf. Ser. **111**, 012051 (2008).
[21] C. -M. Herbach *et al.*, Nucl. Phys. A **712**, 207 (2002).
[22] A. Săndulescu, F. Cărstoiu, Ş. Mişicu, A. Florescu, A.V. Ramayya, J. H. Hamilton, and W. Greiner, J. Phys. G: Nucl. Part. Phys. **24**, 181 (1998).
[23] A. Săndulescu, F. Cărstoiu, I. Bulboacă, and W. Greiner, Phys. Rev. C **60**, 044613 (1999).
[24] Ş. Mişicu, A. Săndulescu, F. Cărstoiu, M. Rizea, and W. Greiner, Nuovo Cimento A **112**, 313 (1999).
[25] F. Cărstoiu, I. Bulboacă, A. Săndulescu, and W. Greiner, Phys. Rev. C **61**, 044606 (2000).
[26] Ş. Mişicu, A. Săndulescu, and W. Greiner, Phys. Rev. C **61**, 041602(R) (2000).
[27] D. N. Poenaru, B. Dobrescu, W. Greiner, J. H. Hamilton, and A. V. Ramayya, J. Phys. G: Nucl. Part. Phys. **26**, L97 (2000).
[28] A. Florescu, A. Săndulescu, D. S. Delion, J. H. Hamilton, A. V. Ramayya, and W. Greiner, Phys. Rev. C **61**, 051602(R) (2000).
[29] J. P. Lestone, Phys. Rev. C **70**, 021601(R) (2004).
[30] A. V. Andreev, G. G. Adamian, N. V. Antonenko, S. P. Ivanova, S. N. Kuklin, and W. Scheid, Eur. Phys. J. A **30**, 579 (2006).
[31] A. V. Andreev, G. G. Adamian, N. V. Antonenko, S. P. Ivanova, and W. Scheid, Rom. Rep. Phys. **59**, 217 (2007).
[32] G. Royer, F. Haddad, and J. Mignen, J. Phys. G: Nucl. Part. Phys. **18**, 2015 (1992).
[33] G. Royer, J. Phys. G: Nucl. Part. Phys. **21**, 249 (1995).
[34] D. N. Poenaru, B. Dobrescu, W. Greiner, J. H. Hamilton, and A. V. Ramayya, J. Phys. G: Nucl. Part. Phys. **26**, L97 (2000).

[35] D. N. Poenaru, W. Greiner, J. H. Hamilton, A. V. Ramayya, E. Hourany, and R. A. Gherghescu, Phys. Rev. C **59**, 3457 (1999).

[36] J. Cseh, J. Phys. G: Nucl. Part. Phys. **19**, L97 (1993).

[37] A. Algora and J. Cseh, J. Phys. G: Nucl. Part. Phys. **22**, L39 (1996).

[38] J. Cseh, A. Algora, J. Darai, and P. O. Hess, Phys. Rev. C **70**, 034311 (2004).

[39] A. Algora, J. Cseh, J. Darai, and P. O. Hess, Phys. Lett. B **639**, 451 (2006).

[40] K. Manimaran and M. Balasubramaniam, Phys. Rev. C **79**, 024610 (2009).

[41] K. Manimaran and M. Balasubramaniam, J. Phys. G: Nucl. Part. Phys. **37**, 045104 (2010).

[42] K. Manimaran and M. Balasubramaniam, Eur. Phys. J. A **45**, 293 (2010).

[43] G. Audi and A. H. Wapstra, Nucl. Phys. A **595**, 4 (1995).

[44] P. Möller, J. R. Nix, W. D. Myers, and W. J. Swiatecki, At. Data Nucl. Data Tables **59**, 185 (1995).